Engineering growing tissues

Eben Alsberg*, Kenneth W. Anderson†, Amru Albeiruti‡, Jon A. Rowley*, and David J. Mooney*‡§¶

Departments of *Biomedical Engineering, †Otolaryngology–Head and Neck Surgery, ‡Biologic and Materials Sciences, and §Chemical Engineering, University of Michigan, Ann Arbor, MI 48109

Edited by Robert Langer, Massachusetts Institute of Technology, Cambridge, MA, and approved July 10, 2002 (received for review May 15, 2002)

Regenerating or engineering new tissues and organs may one day allow routine replacement of lost or failing tissues and organs. However, these engineered tissues must not only grow to fill a defect and integrate with the host tissue, but often they must also grow in concert with the changing needs of the body over time. We hypothesized that tissues capable of growing with time could be engineered by supplying growth stimulus signals to cells from the biomaterial used for cell transplantation. In this study, chondrocytes and osteoblasts were cotransplanted on hydrogels modified with an RGD-containing peptide sequence to promote cell multiplication. New bone tissue was formed that grew in mass and cellularity by endochondral ossification in a manner similar to normal long-bone growth. Transplanted cells organized into structures that morphologically and functionally resembled growth plates. These engineered tissues could find utility in treating diseases and injuries of the growth plate, testing the effect of experimental drugs on growth-plate function and development, and investigating the biology of long-bone growth. Furthermore, this concept of promoting the growth of engineered tissues could find great utility in engineering numerous tissue types by way of the transplantation of a small number of precursor cells.

bone | cartilage | alginate | adhesion ligands | endochondral ossification

A new approach to addressing difficult tissue reconstructive or replacement problems is to engineer new tissues by using selective cell transplantation on polymer scaffolds (1). Functional biologic prostheses are created in this approach by entrapping dissociated cells into synthetic biodegradable polymer substrates that act to deliver the cells to the appropriate anatomic site, define a space for tissue development, and direct the gross size and shape of the engineered tissue (2). This approach has been successful with skin, bone, and cartilage, but a critical unmet challenge is the regeneration of tissues capable of growing over time (e.g., in concert with the growth of a child). One example of a growing tissue is the epiphyseal growth plate, which is responsible for bone elongation during development through a process termed endochondral ossification. Endochondral ossification involves the deposition of osteoid matrix on top of calcified cartilage and its subsequent mineralization (3), and this process is compromised in multiple disease and injury states such as osteochondrodysplasias, epiphyseal osteochondroses, premature growth plate fusion, and Legg–Calve–Perthes disease (4).

We hypothesized that it would be possible to engineer a growing tissue by presenting appropriate growth stimuli from the cell transplantation scaffold. This hypothesis was tested in the context of engineering growing bony tissues by the cotransplantation of osteoblasts and chondrocytes. It is critical to promote the multiplication of transplanted cells if one is to engineer a growing tissue *in vivo*, and one required growth stimulus for most mammalian cell types is an appropriate adhesive substrate (5). We hypothesized that providing a high density of adhesive ligands to transplanted chondrocytes from the polymeric delivery vehicle would promote their multiplication, and synthetic peptides containing the arginine-glycine-aspartic acid (RGD) cell adhesion sequence were covalently coupled to the alginate polymer chains used to form the hydrogel delivery vehicle to provide this requirement. We have previously documented that this approach allows one to specify the mechanism of cell–material adhesion, and that an appropriate density of RGD ligands promotes the proliferation of various cell types *in vitro* (6, 7). Considerable efforts have been made to date to regenerate bone and cartilage tissues separately and together (8–12), but no attempts to form a growing bony tissue have been reported. We now demonstrate it is possible to regenerate a tissue structurally and functionally similar to a growth plate by providing a growing cartilage anlage with transplanted chondrocytes, similar to that in long-bone development, as a framework for subsequent bone formation by cotransplanted osteoblasts.

Methods

Alginate Preparation. MVG alginate was purchased from Pronova Biopolymers (Oslo). The peptide glycine-glycine-glycine-glycine-arginine-glycine-aspartic acid-tyrosine (G_4RGDY) was synthesized at the University of Michigan Protein and Carbohydrate Structure Core facility, and covalently coupled to the alginate as described (6) to yield hydrogels with a final peptide concentration of 1.5×10^5 nmol/liter. Modified alginate was purified with extensive dialysis for 4 days and activated charcoal treatment, and sterilized through a 0.22-μm filter. Control alginate (no peptides) was prepared in a similar manner.

Chondrocyte Transplantation in Alginate Hydrogels and Subsequent Harvest. Severe combined immunodeficient (CB17) mice were purchased (Taconic, Germantown, NY) at 4- 5 weeks of age and used as recipients in all experiments. Freshly slaughtered calf forelimbs were obtained from a local slaughterhouse, and primary bovine articular chondrocytes (BAC) were isolated as described (13). Three experimental conditions were transplanted into mice: (group 1) unmodified alginate alone, without coupled G_4RGDY cell-adhesion ligands and without isolated chondrocytes (negative control group), (group 2) unmodified alginate with isolated chondrocytes, and (group 3) G_4RGDY-coupled alginate with isolated chondrocytes. The appropriate alginate for each group was prepared at a concentration of 2% (wt/wt) by dissolving in PBS, and (in groups 2 and 3) freshly isolated cells were added to yield a cellular density of 30×10^6 cells per ml. Cell-alginate solutions were mixed with aqueous slurries of calcium sulfate (210 mg/ml in ddH_20) in a ratio of 25:1 (7). Fifteen male severe combined immunodeficient mice (CB17) served as recipients for the various polymer–cell implants. After adequate anesthesia of mice was obtained, each animal received three 200-μl s.c. dorsal injections by means of an 18-gauge needle under the dorsal panniculus carnosus. These sites correspond to the distribution of the four large vascular bundles supplying the dorsal skin envelope. Each of the 15 mice supported one injection from each of the experimental groups. The quadrant of the mouse dorsum used for each experimental group injection was rotated with each successive mouse. Mice were killed at 6, 12, and 25 weeks after implantation. The injected constructs were dissected free of surrounding soft tissue, and each of the specimens was palpated with forceps to

This paper was submitted directly (Track II) to the PNAS office.

Abbreviations: BAC, bovine articular chondrocytes; RCO, rat-derived calvarial osteoblasts.

¶To whom reprint requests should be addressed. E-mail: mooneyd@umich.edu.

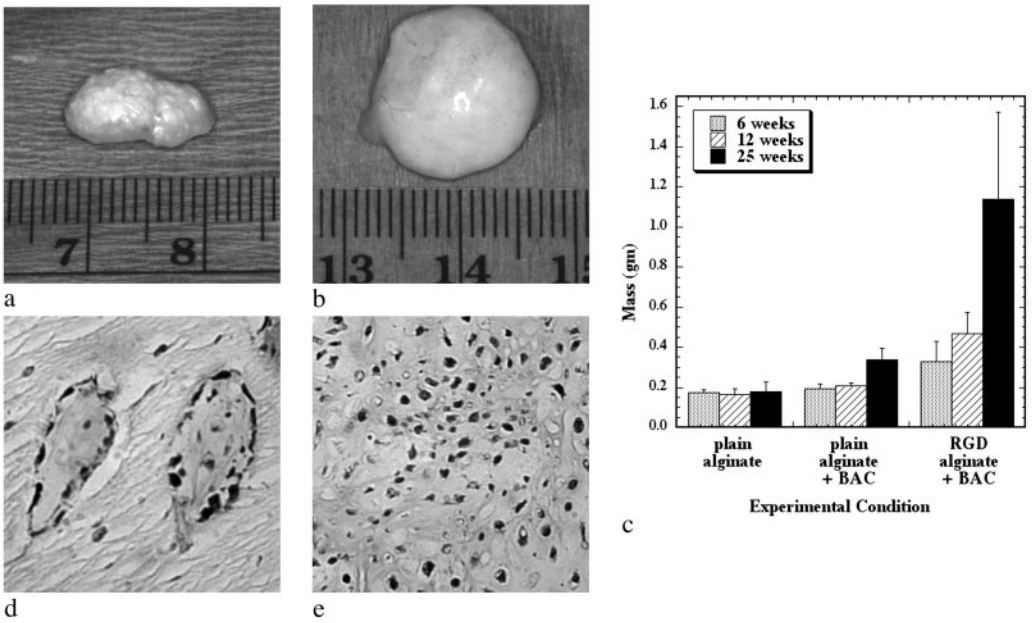

Fig. 1. Growing cartilaginous tissues were engineered with appropriate polymeric delivery vehicles. The gross appearance of chondrocytes transplanted with unmodified alginate (*a*) and RGD-modified alginate (*b*) after 25 weeks, and changes in implant mass over time (*c*) demonstrated growth of the engineered tissue when adhesion ligands are provided by the transplantation vehicle. Masson's Trichrome stain indicating the presence of cross-linked collagen after 6 weeks in the unmodified alginate/chondrocyte group (×100) (*d*) and the RGD-modified alginate/chondrocyte group (×100) (*e*), although the extent of formation of a cartilaginous tissue was accelerated in the RGD-alginate vehicle.

assess clinically mechanical rigidity. Implants were measured and weighed, and biomechanical testing was performed. Each implant was subsequently divided into three equal pieces with a scalpel. One piece was fixed in 10% phosphate-buffered formalin for histologic and immunohistochemical analysis, and the remaining tissues were placed in a −80°C freezer for subsequent analysis of DNA content. National Institutes of Health guidelines for the care and use of laboratory animals have been observed in this and all procedures involving animals.

Histologic Examination of Cartilage Tissues. Specimens were collected and fixed in 10% buffered formalin, dehydrated in increasing concentrations of ethanol, and embedded in paraffin. With use of standard histochemical techniques, serial sections were stained with hematoxylin/eosin and Masson's Trichrome blue at the Histology Core of the University of Michigan Dental School. One histologic section of each implant from the 25-week time point in the study was processed for immunohistochemical staining by using an antibody raised against human type II collagen that cross-reacts with bovine type II collagen and demonstrates no cross-reactivity with other collagen subtypes (I, III, V, and VI) (Biogenesis, Sandown, NH). Sections stained for the presence of type II collagen were analyzed by using Adobe PHOTOSHOP and Scion IMAGE computer image analysis software.

Cotransplantation Experiment and Subsequent Harvest. Rat-derived calvarial osteoblasts (RCO) were isolated from newborn (<3 days old) Lewis rat pups (pregnant Lewis rats were purchased from Harlan–Sprague–Dawley) by using a reported method (14). Two experimental groups were investigated: (*i*) primary RCO cells alone, and (*ii*) a 2:1 ratio of RCO cells to BAC cells, keeping the transplantation cell number constant in both conditions. The cells were mixed with alginate solutions (2% wt/wt in PBS; $G_4RGDY = 1.5 \times 10^5$ nmol/liter) to achieve a final total cell concentration of 39.4×10^6 cells per ml, and the cell-alginate solutions were mixed with aqueous slurries of calcium sulfate (7). Two hundred microliters of each of the two experimental groups was injected through an 18-gauge needle s.c. into the backs of 4- to 5-week-old anesthetized severe combined immunodeficient mice. Although no mice were lost during the surgeries, one mouse died at an intermediate time point and was not analyzed, and two mice died of unknown causes within a few days of their respective time points and were analyzed. The implants were harvested after 4 ($n = 4$), 13 ($n = 5$), and 26 ($n = 4$–5) weeks. Entire specimen masses were measured, dual-energy x-ray absorptiometric images were scanned to determine bone mineral density and content, the specimens were cut into thirds, and the masses of the thirds were measured. One-third was fixed in formalin, embedded in paraffin, sectioned, and stained by using a standard hematoxylin/eosin protocol and a standard aldehyde fuchsin/alcian blue and eosin protocol for microscopic observation and histomorphometric analysis of total bone, cartilage, marrow space, fibrous tissue, and alginate fraction in one section from each implant at 26 weeks ($n = 4$–5 per group). The other two-thirds were flash-frozen in liquid nitrogen and stored at −80°C for later DNA analysis.

DNA Analysis. The number of cells in explanted tissues at each time point was determined by measuring the amount of DNA in enzyme-digested samples by using Hoechst 33258 dye and a fluorometer (Hoefer DyNA Quant 200, Amersham Pharmacia) as described (15). DNA quantities were converted to cell numbers by using a conversion factor of 8 pg of DNA per cell (16).

Statistics. Statistical analysis was performed by paired one-tailed Student's *t* test except for comparisons between different time points, in which case the unpaired one-tailed alternate Welsh *t* test was performed. Statistical significance was considered at $P < 0.05$.

Results and Discussion

To test first if a growing cartilaginous tissue could be engineered, as a first step to engineering growing bony tissues, RGD-modified and unmodified alginate hydrogels were used to trans-

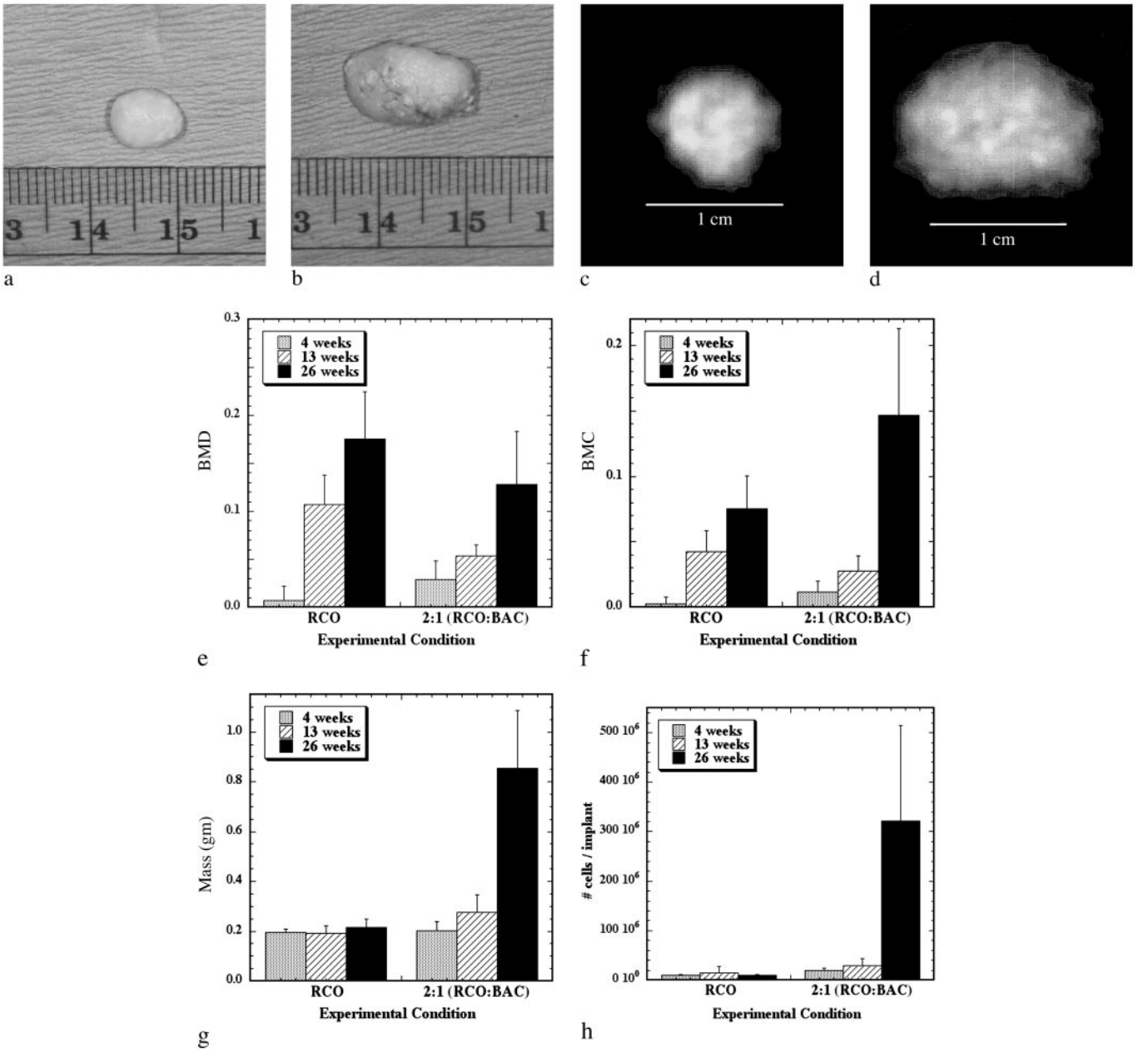

Fig. 2. Engineering bony tissues with osteoblast and chondrocyte cotransplantation results in an increased mass, mineral content, and cellularity with time, as contrasted to osteoblast-alone transplantation. Gross appearance and dual-energy x-ray absorptiometric images at 26 weeks of implants resulting from transplantation of RCO cells only (*a* and *c*), and a 2:1 ratio of RCO to BAC cells (*b* and *d*) in an RGD-modified alginate qualitatively demonstrated increased implant size and mineral content as a result of cotransplantation. Quantification of changes in bone mineral density (e) and bone mineral content (*f*) indicated significantly greater bone mineral content in the implants containing a 2:1 ratio of BAC cells to RCO cells compared with the condition with RCO cells only at 4 and 26 weeks. Plots of implant mass (*g*) and total cell number (*h*) over time revealed significant increases over time only in the cotransplantation group. The mass and total number of cells of the cotransplantation group were significantly greater than the RCO-only group at 26 weeks. Within the cotransplantation group, masses and total number of cells were significantly greater at 26 weeks than at 4 and 13 weeks.

plant isolated chondrocytes into mice for periods from 6 to 25 weeks. Gross examination of explanted tissues revealed that only implants combining chondrocytes with RGD-alginate demonstrated convincing characteristics similar to native cartilage (e.g., pearly white opalescence, firm to palpation) (Fig. 1 *a* and *b*). Furthermore, tissues engineered with the RGD-modified alginate increased significantly in mass (Fig. 1*c*) and size over time. Quantification of the cell number in these tissues indicated a continued increase in cell number over time (data not shown), supporting the gross observation of extensive tissue growth.

Histologic evaluation of the engineered tissues indicated an accelerated rate of tissue formation (e.g., higher cellularity and type II collagen deposition, decreased residual alginate) with the RGD-alginate hydrogels. The negative control group (unmodified alginate without cells) demonstrated only residual alginate and fibrovascular ingrowth; no evidence of cartilage formation was exhibited by any of these implants at any time. Implants of unmodified alginate with chondrocytes demonstrated islands of cartilage-like tissue (Fig. 1*d*) that were noted to expand and coalesce with increasing time of implantation. In contrast,

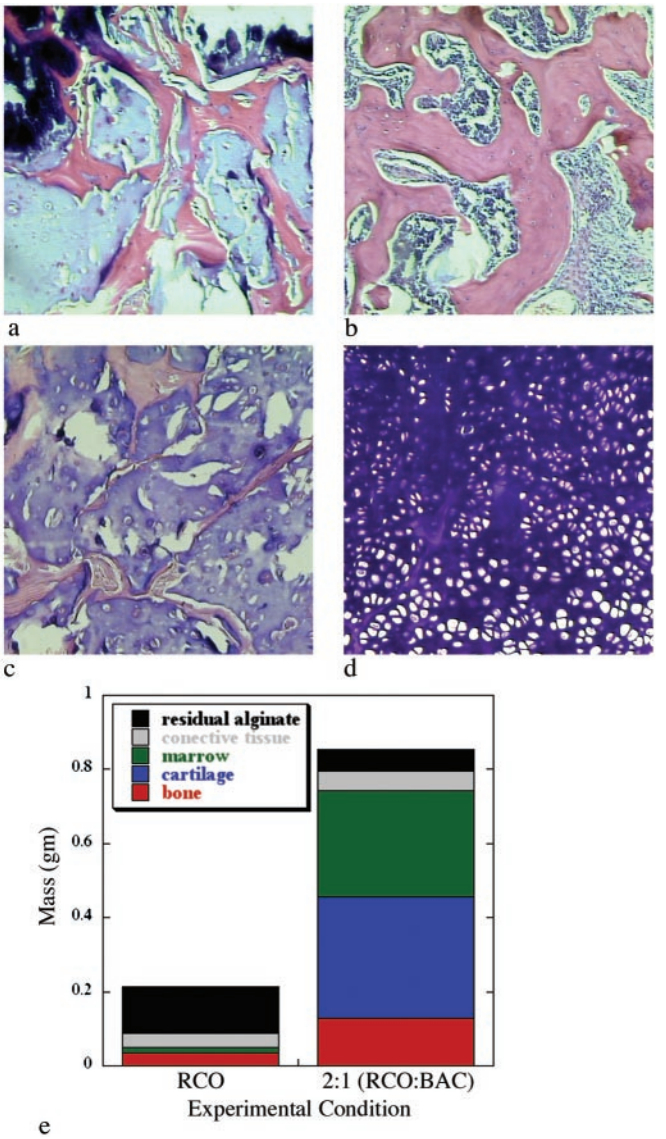

Fig. 3. Tissues composed of both bone and cartilage were engineered through cotransplantation. Hematoxylin/eosin-stained sections demonstrate mature bone formation at 26 weeks in implants consisting of alginate-RGD mixed with RCO cells (*a*), and a 2:1 ratio of RCO to BAC cells (*b*), although substantial marrow space was observed only in the cotransplantation group (×100). Aldehyde fuchsin/alcian blue and eosin staining of sections revealed only residual alginate in the RCO-only implants (*c*). In contrast, an abundant, highly cellular cartilaginous matrix was observed in the 2:1 cotransplantation implants (*d*) at 26 weeks (×100). Histomorphometric quantification of implant tissue compositions (*e*) clearly depicts substantial cartilage formation in the cotransplantation group, and significantly more bone and marrow space in these engineered tissues, compared with the RCO-only control.

implants of RGD-alginate with chondrocytes demonstrated an abundance of cartilage-like tissue even at the earliest time point, with small islands of residual alginate contained within the cartilage (Fig. 1*e*). The ratio of cartilage to alginate increased with time, and at the 25-week time point these implants were almost entirely composed of cartilage-like tissue, with only occasional small pockets of residual alginate. Quantification of the areas staining positive for type II collagen (a specific marker for cartilage), by using computerized image analysis, revealed that the negative control demonstrated no type II collagen deposition. In contrast, the RGD-alginate group exhibited extensive positive staining (95 ± 3% of tissue area). These tissues also demonstrated significantly greater compressive moduli than tissues engineered with unmodified alginate (data not shown), further supporting the finding of increased rate of cartilage formation. Significant progress has been made toward engineering functional cartilage tissue in terms of achieving mechanical, biochemical, and histologic properties similar to those properties of native cartilage (17); however, no growing cartilage tissue has been reported previously. The current findings demonstrate that providing specific cell-adhesive interactions with the cell delivery vehicle can markedly enhance the growth of engineered cartilage tissue.

Once a growing cartilage template had been achieved, the cellular environment present during endochondral ossification was partially recreated in an effort to form a tissue engineered growth plate-like structure. Past studies aimed at modeling growth plate physiology used monolayer chondrocyte cultures, which do not stabilize the chondrocyte phenotype and neglect the true *in vivo* spatial arrangement of chondrocytes and their matrix (18, 19). Subsequent studies have used chondrocyte aggregates (20) or suspension cultures in which chondrocytes were cultured in a variety of three-dimensional gels (21–27). Although these systems preserved the chondrocyte rounded phenotype and provided a more realistic three-dimensional environment, none of these models provided for chondrocyte transformation from a proliferative to a differentiating phenotype within the growth plate (20) nor accounted for the complex cell–cell interactions and soluble signaling that occurs between osteoblasts and chondrocytes within an actual growth plate. To address these limitations of past models, chondrocytes and osteoblasts were mixed together in a G_4RGDY-modified alginate delivery vehicle and injected into the backs of severe combined immunodeficient mice for 4–26 weeks. A control of osteoblasts-alone transplantation was also used in this study. Engineered tissues were excised at 26 weeks, and gross inspection of both experimental groups revealed the appearance of bony nodules (Fig. 2 *a* and *b*). Specimens with a 2:1 ratio of primary RCO to primary BAC cells were substantially larger than the RCO-only transplants, however, and also had regions that grossly resembled cartilage. Bone mineral density plots taken with dual-energy x-ray absorptiometric imaging on implants at 26 weeks confirmed mineral content throughout the implants in both groups (Fig. 2 *c* and *d*). Although the bone mineral density was significantly greater in the RCO-only group than in the cotransplantation group at 13 and 26 weeks (Fig. 2*e*), the bone mineral content in the cotransplantation group was significantly greater than that of the RCO-only group at 4 and 26 weeks (Fig. 2*f*). In addition, the mass (Fig. 2*g*) and the cell number per implant (Fig. 2*h*) of the cotransplantation group significantly increased over time, while no increase in either variable was observed in the RCO cell-only condition over time. Thus, cotransplantation of chondrocytes and osteoblasts in this vehicle resulted in a growing bony tissue, as evidenced by significantly increased mineral content, mass, and cell density over time.

Histologic examination of the RCO cell only and cotransplantation constructs revealed mature bone formation in both conditions at 26 weeks (Fig. 3 *a* and *b*). The cartilage, however, was present only in the cotransplantation group, as confirmed both morphologically and through specific staining of sulfated mucopolysaccharides (component of cartilage) (Fig. 3 *c* and *d*). Histomorphometric analysis of hematoxylin/eosin and aldehyde fuchsin/alcian blue/eosin-stained sections, by using image analysis software, revealed that the total amount of bone achieved with cotransplantation of the two cells types was significantly greater than that obtained from the transplantation of RCO cells alone (Fig. 3*e*). In addition, unlike the RCO-only group, the cotransplantation group demonstrated significant cartilage tis-

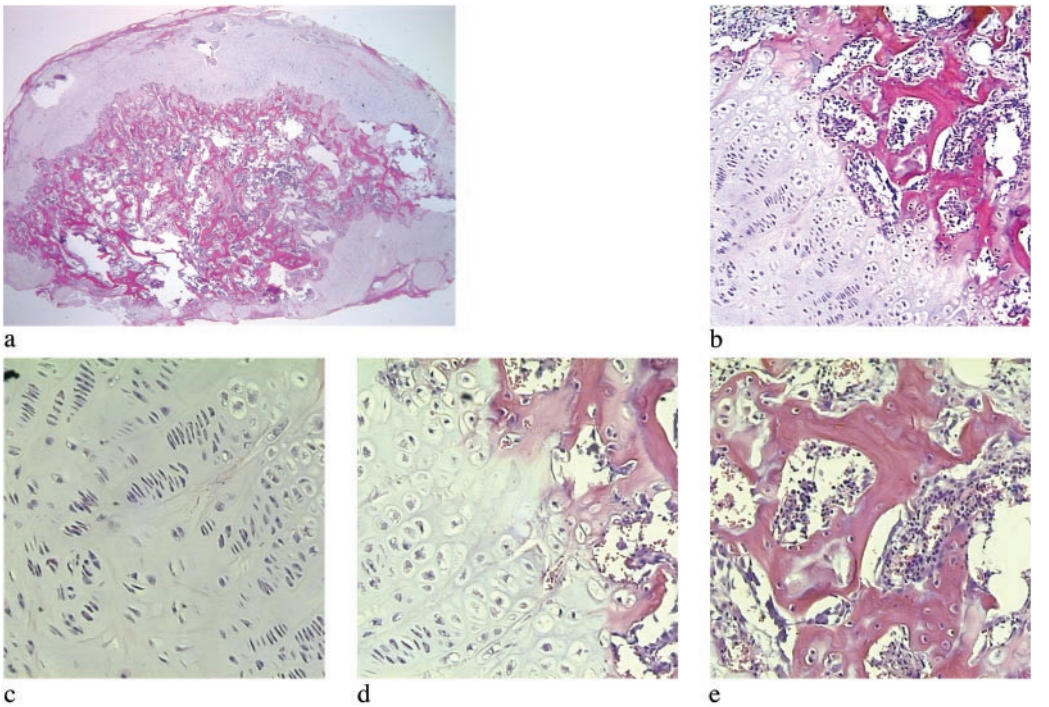

Fig. 4. Cotransplantation in the RGD-vehicle provided the necessary signals for the formation of growth-plate-like structures. Low magnification of a histologic section indicates the macroscopic organization of the growth-plate-like structures (*a*) (×20). Examination of the interface between cartilaginous and bony regions of tissues engineered with cotransplanted osteoblasts and chondrocytes demonstrated a structure (*b*) similar to that seen in developing long bones (×100). Magnification of the cartilage (*c*), transition (*d*), and bone and marrow space (*e*) regions demonstrated cellular and tissue morphology typical of the corresponding regions in a growth plate (×200).

sue and marrow space. Minimal alginate remained in the cotransplantation group, whereas more than 50% of the tissue in the RCO-only group was residual carrier.

A striking result observed in the cotransplantation group was that 80% of these growing bony tissues contained structures that histologically resembled growth plates (Fig. 4 *a* and *b*) at the interface of the cartilaginous and bony regions of the tissue. The first region of these structures is similar to the reserve zone of normal growth plate histology, where the spherical chondrocytes exist individually or in pairs and are similar in size to the cells of the proliferative zone (Fig. 4*c*). These chondrocytes are separated by large amounts of extracellular matrix and not as densely packed as cells in the other regions (28). In the next region, the chondrocytes, flattened and aligned in longitudinal columns, mirror the morphology of the proliferative zone of the growth plate (Fig. 4*c*) (29). The flattened cells of the preceding region turn into rounded, distended chondrocytes, which are similar in morphology to the hypertrophic zone of a growth plate (Fig. 4*d*). The final region exhibits trabeculae of primary spongiosa and marrow space typical of a growth plate's metaphysis (Fig. 4*e*) (3). The regions of cartilaginous and bony tissues ranged in size from $\approx$1.75 to 11.50 mm^2, with the junctions between the zones ranging from $\approx$1 to 6.5 mm. Organization of transplanted cells to form growth-plate-like structures has not been reported, but other cell types (30–36) have demonstrated the ability to self-assemble *in vitro* into structures that have similar functional and/or morphological properties to the tissues from which they were isolated (37). In addition, several groups have engineered complex functional tissues such as the urinary bladder (38) and the small intestine (39) through the transplantation of multiple cell types in specific locations on the delivery vehicle. However, the development of growth-plate-like structures presented here is a striking demonstration of the ability of randomly mixed multiple cell types to self-organize into several distinct tissue types. The mechanisms of cellular self-assembly underlying these findings are not entirely understood, but may include differential adhesion between different cell types, differential response to chemotactic gradients, different rates of adhesiveness reacquisition after cell isolation, the differential contractility hypothesis, and the specific adhesion hypothesis (40). The different cell types may also affect the organization of each other by the secretion of growth factors, or the cell populations may respond differently to the insoluble signals provided by the adhesive moiety bonded to the alginate vehicle.

The results of these studies may have direct therapeutic applications and provide a model system to study normal and pathologic processes of bone formation. Although the transplantation of viable epiphyses to treat growth disorders in children is an attractive therapy, it is problematic because of a lack of excess autologous growth plate cartilage sites and immunological problems associated with allografts. In addition, weight-bearing large animal epiphyseal transplant models have not been successful to date (41). These types of engineered constructs may potentially be used to replace dysfunctional epiphyses. In addition, significant advances have been made in elucidating the genetic basis of various congenital skeletal diseases, such as those resulting in abnormal growth plate function (42), and the effects of drug interventions for these diseases may be investigated with this system before utilization in clinical trails. Important issues in either application of this system will be the optimization of the rate of growth plate formation and the location of the structures. Variations in construct oxygen tension may also be manipulated to regulate the spatial orientation and distribution of the different cell populations, because this variable plays an important role in the different zones of the growth plate *in vivo* (28). Finally, it may be possible to predefine precisely the placement of individual cell populations within a three-

dimensional delivery vehicle via micropatterns of self-assembled monolayers, polymers, extracellular matrix proteins, or cell-adhesion peptides (43) to control the development of the structures.

This approach to tissue engineering, transplantation of a small number of cells and growing the tissue *in vivo*, may profoundly affect this field. First, this approach may bypass current difficulties in the *in vitro* engineering of large tissue masses for subsequent transplantation that are related to a lack of vascularity and large-scale cell death (44). Second, this approach may be ideal for the utilization of small numbers of stem cells in the regeneration of various tissues in the body.

We thank Dr. Evan T. Keller for the use of his dual-energy x-ray absorptiometer and Boyer's Meat Processing (Canton, MI) for supplying the calves. D.J.M. received funding from the National Institute of Dental and Craniofacial Research (R01-DE13033). E.A. was supported by National Institute of Dental and Craniofacial Research Graduate Fellowship T32-DE07057, K.W.A. was supported by National Institutes of Health Training Grant T32-DC05356, and J.A.R. was supported by National Institutes of Health Training Fellowship GM08353.

1. Langer, R. & Vacanti, J. P. (1993) *Science* **260,** 920–926.
2. Putnam, A. J. & Mooney, D. J. (1996) *Nat. Med.* **2,** 824–826.
3. Jee, W. S. S. (1987) in *Histology: Cell and Tissue Biology*, ed. Weiss, L. (Elsevier, New York), pp. 212–254.
4. Beers, M. H., Berkow, R. & Burs, M., eds. (1999) *The Merck Manual of Diagnosis and Therapy* (Merck, Rahway, NJ), 17th Ed.
5. Peppas, N. A. & Langer, R. (1994) *Science* **263,** 1715–1720.
6. Rowley, J. A., Madlambayan, G. & Mooney, D. J. (1999) *Biomaterials* **20,** 45–53.
7. Alsberg, E., Anderson, K. W., Albeiruti, A., Franceschi, R. T. & Mooney, D. J. (2001) *J. Dent. Res.* **80,** 2025–2029.
8. Nakahara, H., Goldberg, V. M. & Caplan, A. I. (1992) *Clin. Orthop. Relat. Res.* **276,** 291–298.
9. Iyoda, K., Miura, T. & Nogami, H. (1993) *Clin. Orthop. Relat. Res.* **288,** 287–293.
10. Ishaug, S. L., Yaszemski, M. J., Bizios, R. & Mikos, A. G. (1994) *J. Biomed. Mater. Res.* **28,** 1445–1453.
11. Isogai, N., Landis, W., Kim, T. H., Gerstenfeld, L. C., Upton, J. & Vacanti, J. P. (1999) *J. Bone Jt. Surg. Am. Vol.* **81,** 306–316.
12. Alsberg, E., Hill, E. E. & Mooney, D. J. (2001) *Crit. Rev. Oral Biol. Med.* **12,** 64–75.
13. Paige, K. T., Cima, L. G., Yaremchuk, M. J., Vacanti, J. P. & Vacanti, C. A. (1995) *Plast. Reconstr. Surg.* **96,** 1390–1400.
14. Pockwinse, S. M., Wilming, L. G., Conlon, D. M., Stein, G. S. & Lian, J. B. (1992) *J. Cell Biochem.* **49,** 310–323.
15. Kim, Y. J., Sah, R. L., Doong, J. Y. & Grodzinsky, A. J. (1988) *Anal. Biochem.* **174,** 168–176.
16. Shea, L. D., Wang, D., Franceschi, R. T. & Mooney, D. J. (2000) *Tissue Eng.* **6,** 605–617.
17. Martin, I., Obradovic, B., Treppo, S., Grodzinsky, A. J., Langer, R., Freed, L. E. & Vunjak-Novakovic, G. (2000) *Biorheology* **37,** 141–147.
18. Kuettner, K. E., Pauli, B. U., Gall, G., Memoli, V. A. & Schenk, R. K. (1982) *J. Cell Biol.* **93,** 743–750.
19. Jikko, A., Aoba, T., Murakami, H., Takano, Y., Iwamoto, M. & Kato, Y. (1993) *Dev. Biol.* **156,** 372–380.
20. Farquharson, C. & Whitehead, C. C. (1995) *In Vitro Cell. Dev. Biol. Anim.* **31,** 288–294.
21. Benya, P. D. & Shaffer, J. D. (1982) *Cell* **30,** 215–224.
22. Aigner, J., Tegeler, J., Hutzler, P., Campoccia, D., Pavesio, A., Hammer, C., Kastenbauer, E. & Naumann, A. (1998) *J. Biomed. Mater. Res.* **42,** 172–181.
23. Horton, W. & Hassell, J. R. (1986) *Dev. Biol.* **115,** 392–397.
24. Sims, C. D., Butler, P. E., Cao, Y. L., Casanova, R., Randolph, M. A., Black, A., Vacanti, C. A. & Yaremchuk, M. J. (1998) *Plast. Reconstr. Surg.* **101,** 1580–1585.
25. Gibson, G. J., Schor, S. L. & Grant, M. E. (1982) *J. Cell Biol.* **93,** 767–774.
26. Kim, W. S., Vacanti, J. P., Cima, L., Mooney, D., Upton, J., Puelacher, W. C. & Vacanti, C. A. (1994) *Plast. Reconstr. Surg.* **94,** 233–240.
27. Guo, J. F., Jourdian, G. W. & MacCallum, D. K. (1989) *Connect. Tissue Res.* **19,** 277–297.
28. Brighton, C. T. (1978) *Clin. Orthop. Relat. Res.* **136,** 22–32.
29. Iannotti, J. P., Goldstein, S., Kuhn, J., Lipiello, L. & Kaplan, F. S. (1994) in *Orthopaedic Basic Science*, ed. Simon, S. R. (Am. Acad. Orthopaedic Surgeons, Rosemont, IL), pp. 185–217.
30. Barcellos-Hoff, M. H., Aggeler, J., Ram, T. G. & Bissell, M. J. (1989) *Development (Cambridge, U.K.)* **105,** 223–235.
31. Shannon, J. M., Mason, R. J. & Jennings, S. D. (1987) *Biochim. Biophys. Acta* **931,** 143–156.
32. Halban, P. A., Powers, S. L., George, K. L. & Bonner-Weir, S. (1987) *Diabetes* **36,** 783–790.
33. Kubota, Y., Kleinman, H. K., Martin, G. R. & Lawley, T. J. (1988) *J. Cell Biol.* **107,** 1589–1598.
34. Denker, A. E., Nicoll, S. B. & Tuan, R. S. (1995) *Differentiation (Berlin)* **59,** 25–34.
35. Kale, S., Biermann, S., Edwards, C., Tarnowski, C., Morris, M. & Long, M. W. (2000) *Nat. Biotechnol.* **18,** 954–958.
36. Landry, J., Bernier, D., Ouellet, C., Goyette, R. & Marceau, N. (1985) *J. Cell Biol.* **101,** 914–923.
37. Tzanakakis, E. S., Hansen, L. K. & Hu, W. S. (2001) *Cell Motil. Cytoskeleton* **48,** 175–189.
38. Oberpenning, F., Meng, J., Yoo, J. J. & Atala, A. (1999) *Nat. Biotechnol.* **17,** 149–155.
39. Kim, S. S., Kaihara, S., Benvenuto, M. S., Choi, R. S., Kim, B. S., Mooney, D. J. & Vacanti, J. P. (1999) *J. Surg. Res.* **87,** 6–13.
40. Armstrong, P. B. (1989) *Crit. Rev. Biochem. Mol. Biol.* **24,** 119–149.
41. Manfrini, M., Randolph, M. A., Andrisano, A. & Weiland, A. J. (1988) *Microsurgery* **9,** 242–245.
42. Mundlos, S. & Olsen, B. R. (1997) *FASEB J.* **11,** 125–132.
43. Folch, A. & Toner, M. (2000) *Annu. Rev. Biomed. Eng.* **2,** 227–256.
44. Peters, M. C., Isenberg, B. C., Rowley, J. A. & Mooney, D. J. (1998) *J. Biomater. Sci. Polym. Ed.* **9,** 1267–1278.